Cutting Zone Temperature and Specific Cutting Energy Measurement and Evaluation in Machining Metals

Y. Yifrach[1], U. Ben-Hanan[2]
[1] Department of Mechanical Engineering, ORT Braude College, P.O. Box 78, Karmiel 21982, Israel
[2] Department of Mechanical Engineering, ORT Braude College, P.O. Box 78, Karmiel 21982, Israel
Email: yifrach@braude.ac.il

Abstract The knowledge of the temperature that develops between tools and the raw material is needed for optimizing the cutting parameters. A controlled Grinding experiment was compared with a thermo-mechanical finite elements model (FEM) simulating the temperature distributions and other effects occurring in the cutting zone. An electric Grinding was controlled by [Labview] software, keeping the torque and rotational speed constant and preventing disruption of fixed air flow.
The processed material was glass ceramics, the mechanical and thermal properties of which are known from the literature. A finite elements model was developed and its parameters determined by matching the computed Nodes with thermocouples' temperature measurements. The experiment was carried out by single slot cutting, without cooling. The value of cutting power was based on specific cutting energy (U), known from the literature and calculation of (MRR) from the cutting parameters (depth & width of cut, feed rate). The dynamic model simulated the movement of cutting tool by sampling heat sources along the path. The fit obtained between dynamic model and the measurements enables a reliable calculation of the specific cutting energy (U) for every combination of tool cut and raw material.

Keywords: cutting, specific cutting energy (U), Material removal rate (MRR), finite element method (FEM).

1. Introduction

Most of the energy of machining is transformed to heat. The heat transfer from the cutting zone depends on the heat capacity of the raw material and on its configuration. The temperature rise of the cutting zone may limit the cutting speed and cutting depth, causing tool wear and limiting its life, and creating thermal stress in the raw material and distortions of its surface.
It is therefore highly desirable to measure the cutting zone temperature and relate it to the cutting performance parameters (depth of cut, cutting velocity, feed, linear speed of cutting progress, power required, Specific Grinding Energy). Due to the nature of metal cutting, it is not possible to measure temperature directly in the cutting zone.
The main techniques used to evaluate the surface temperatures during machining are Thermocouple method and infrared photographic technique [1-4]. Two arrays of thermocouples were lined along both sides of the cutting path for measuring the temperature development throughout the working piece according to the drill's advancement in recent years; the finite element method has particularly become the main tool for simulating metal cutting processes. It is especially important that FEM analysis can help to investigate the temperature distributions and other effects occurring in the

cutting zone. A finite element (FEM) thermal analysis program (NASTRAM software) was developed and reported here, utilizing a moving heating source model [5-6]. In that model, the grinding zone is assumed as a band source of heat that moves along the upper surface of the workpiece. The heat to the Workpiece in dry grinding was calibrated by matching between experimental data using an embedded thermocouples and FEM analysis temperature response. The FEM is used for extrapolation the temperature data from the measured points to the cutting zone.

2. Data acquisition system

The data acquisition system consists of controller, amplifier, A/D convertor, and LabVIEW (Laboratory Virtual Instruments Engineering Workbench) for windows software developed by National Instruments. Once the program runs, thermocouples' temperature and normal grinding force were collected and recorded on an Excel file.

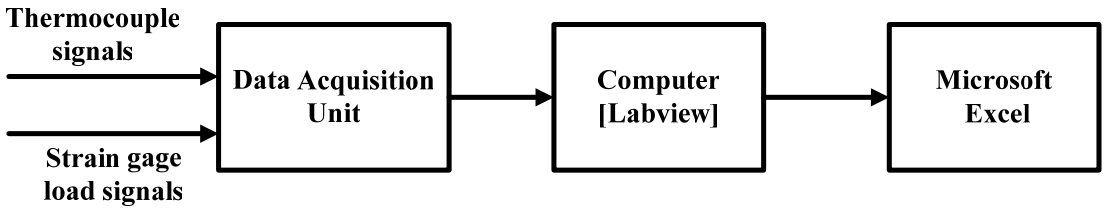

Figure 1. Schematic representation of Data acquisition system

3. Calibration experiment versus finite elements model

The thermal analysis model utilizes parameters from the literature (specific heat capacity, Thermal conductivity and Density).The objective of calibration experiment is to verify the model and calibrate the parameters by matching the results with measurements.

A solder-iron served as a heat source. It was placed at the center of the plate (x=0;y=39mm). An equally-spaced array of four thermocouples was placed in the upper surface and another two thermocouples – on the lower surface (Figure 4).

The temperature at each thermocouple was measured after they reached a steady-state, 450 seconds after the initiation of the heat source (Figure 9). Plots of y-cut temperature distribution at each thermocouple's position were calculated by the model (Figure 6). The ratio of the values at the peaks (locations of the thermocouples) matched the ratio of the measured values at the respective thermocouples. Values of (h) were then iterated in the model to reach a match with the measurements for $h_{final} = 2.0 \cdot 10^{-4} \left[{}^{W}\!/_{mm^2 \cdot {}^0C} \right]$. This is exhibited in Figure 6.

The temperature evolution with time (as measured and displayed Figure 8) was then compared with a time evolution run of the model (Figure 9), which shows a good match.

It is then easy to estimate the heat transfer coefficient (h) after calibrating the finite elements model, for every combination of tool cut and raw material.

3.1. Calibration model of ceramic plate mesh

The full model was built with Solid elements. The dimensions of the plate are 78x78x5 mm. The mesh of the plate model consists of identical elements, with the size of 1x1x1 mm. The total amount of elements in the plate is 30420

3.2. Experimental set-up

The experiment set up and workpiece are described in Figure 2 and Figure 3. It should be noted that this experimental setup is in use for measuring dental bur wear research [5].

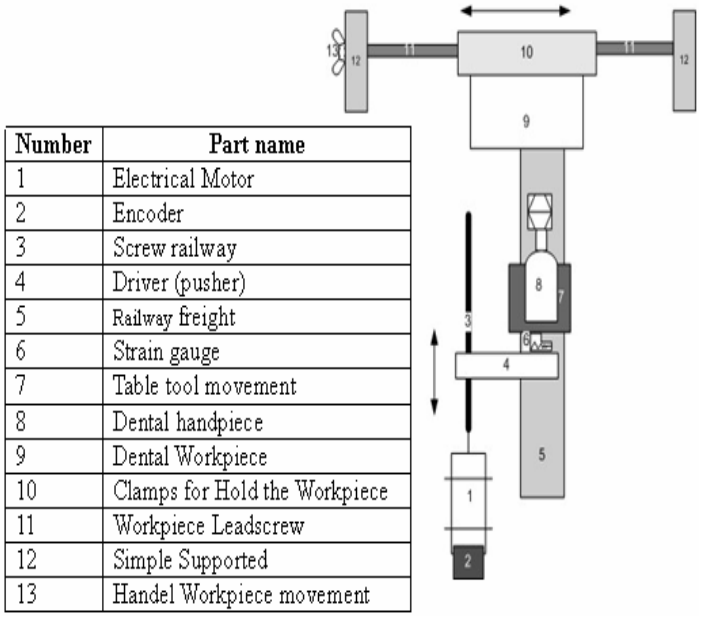

Number	Part name
1	Electrical Motor
2	Encoder
3	Screw railway
4	Driver (pusher)
5	Railway freight
6	Strain gauge
7	Table tool movement
8	Dental handpiece
9	Dental Workpiece
10	Clamps for Hold the Workpiece
11	Workpiece Leadscrew
12	Simple Supported
13	Handel Workpiece movement

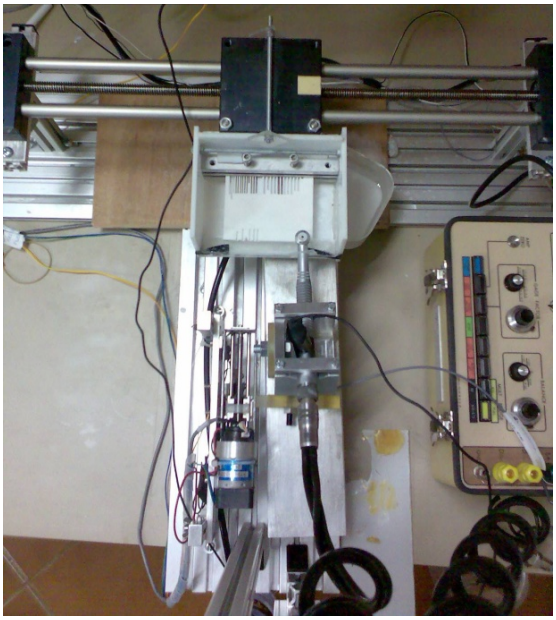

Figure 2. Schematic representation and photo of Experimental set-up

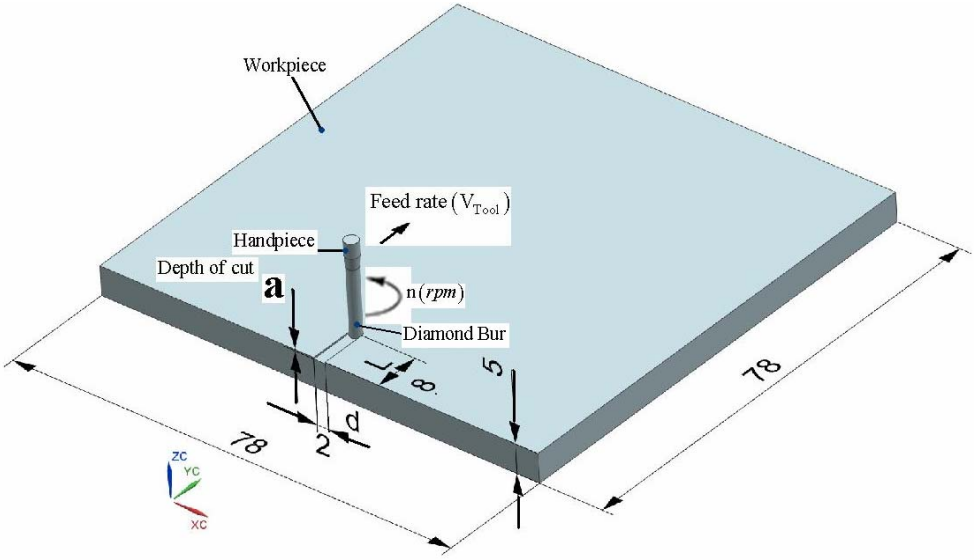

Figure 3. Detailed illustration of the bur- Dental Workpiece movement

3.3. Boundary conditions for calibration static (steady-state) model

(1) The temperature of the heat source is 330°C
(2) The other surfaces that without contact with the heat source will with Convection region.

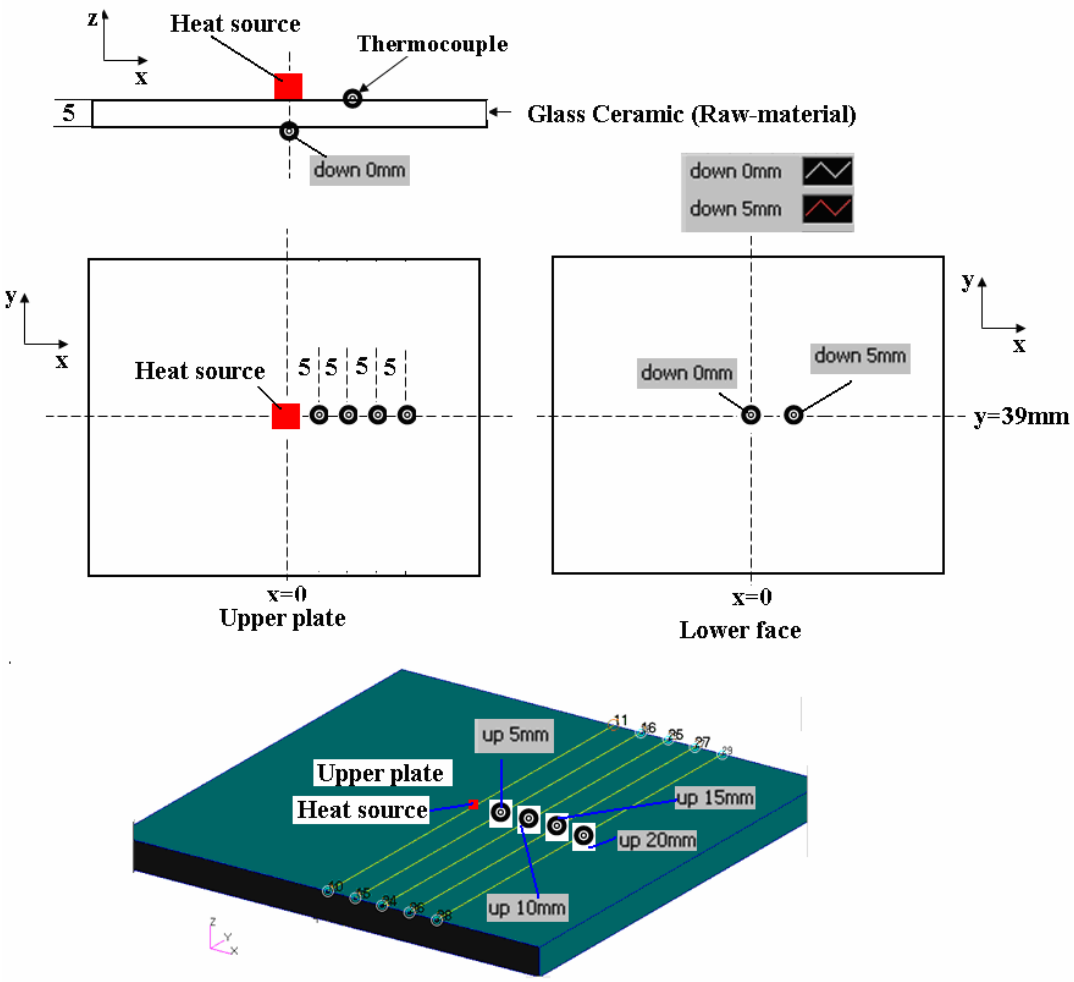

Figure 4. Experiment configuration of thermocouples for measuring the temperature

The convection is assumed to have a small impact on the heat distribution. A fixed heat transfer coefficient (h) is therefore assumed over the working piece. It was estimated (h_{final}) by varying the parameters of the analytical results to match with the measured ones at the thermocouples.
The thermal properties of the ceramic plate (Table 1) were given to the calibrate model and to the grinding model.

Table 1. Thermal properties of the ceramic plate

Material	Thermal conductivity	Specific heat	Density
Machinable Ceramic	$k = 1.46 \cdot 10^{-3} \left[{}^{w}/_{mm \cdot {}^{0}C} \right]$	$c_p = 790 \left[{}^{J}/_{Kg \cdot {}^{0}C} \right]$	$\rho = 2520 \left[{}^{Kg}/_{m^3} \right]$

3.4. Model calibration static results

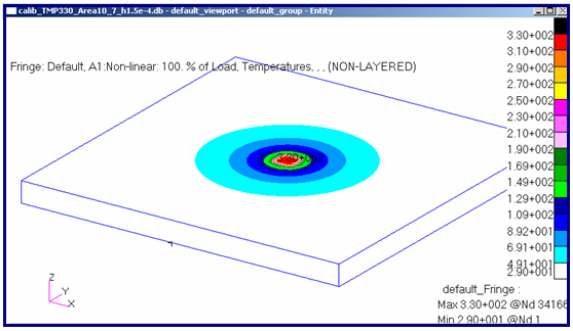

Figure 5. The temperature distribution on the upper surface

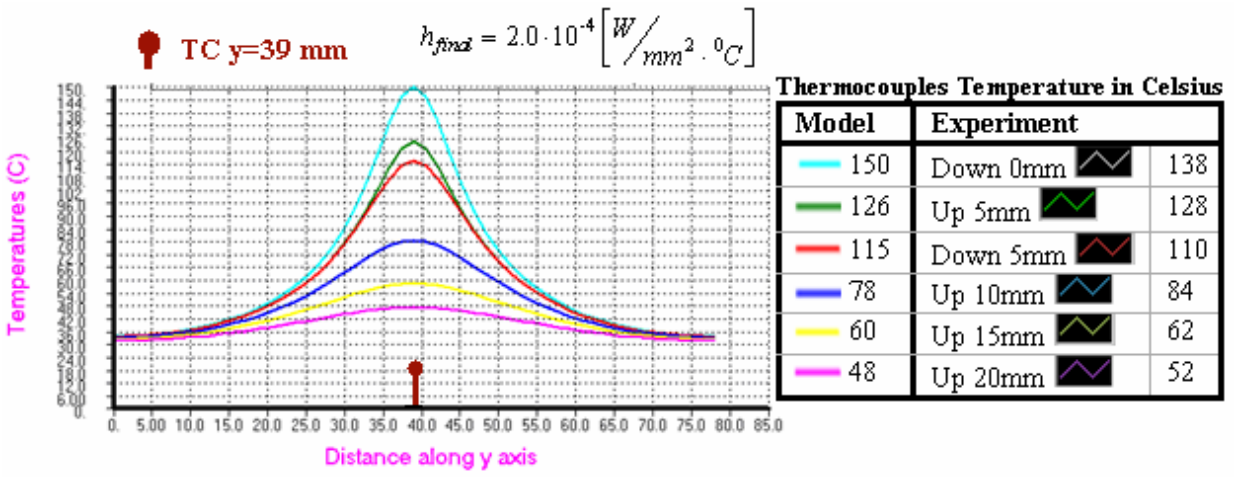

Figure 6. The temperature distribution along y axis on the lower and upper surface

Due to the symmetry of the problem in terms of geometry, loads (heat source) and boundary condition (there is no convection across symmetrical planes) we built a quarter-plate model and thereby save calculation time. A fine-mesh was built near the heat source to capture the delicate changes (Figure 7) so that the gradient temperature through the thickness of the plate is exhibited clearly. It should be noted that the quarter model results are the same as the complete model (described in Figure 5 and 6).

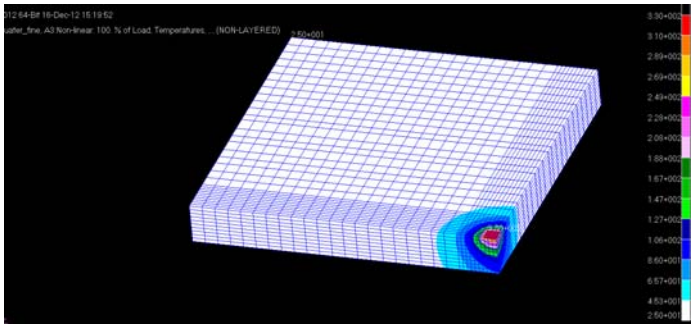

Figure 7. The distribution and size of the temperature on the quarter model, described with fine mesh near the heat source

3.5. Results and discussion from Calibration experiment versus finite elements model

(1) We can see that the temperatures distribution is identical in all curves and received an excellent match with the experiment temperature in stable condition (Figure 6) and (Figure 8).

(2) In this experiment and FEM model the thickness of the plate is relatively small, so the temperature will be higher in the lower-surface (under the heat source) and not on the upper face within 5 mm from the heat source, since the heat dispersed faster in radial direction than in the depth plate direction.

3.6. FEM dynamic model (transient) for calibration

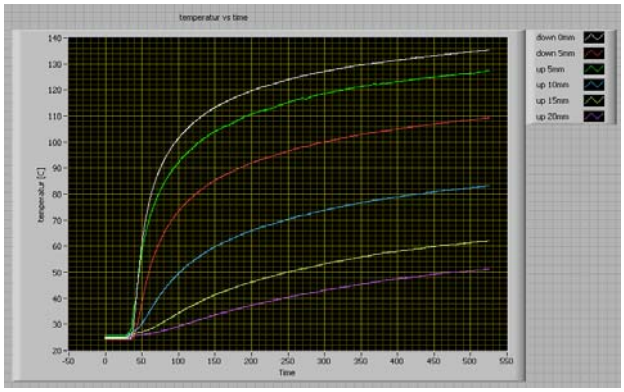

Figure 8. Experimental temperature results versus time of six thermocouples

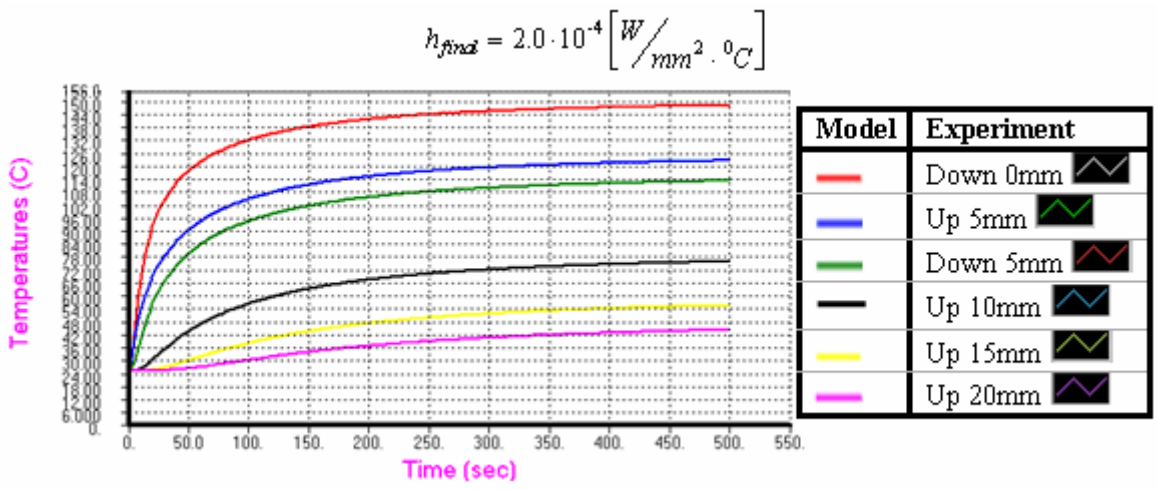

Figure 9. Transient model temperature results versus time of six thermocouples

3.7. Results and discussion of model (transient) for calibration

(1) Receiving in the model and experiment the same distribution temperature in six thermocouples.

(2) Steady state condition of the temperature in each thermocouples nodes in the model is accepted after about 500 seconds and received an excellent match with the experiment temperature in stable condition

(3) Conclusion: There is good reliability in measuring temperature with thermocouples.

4. Grinding experiment without internal or external cooling

The objectives of the experiment are: measuring the temperature of the workpiece in grinding without cooling and calibrating by matching between experimental data, using embedded thermocouples, and FEM analysis temperature response. The FEM is used for extrapolation of the temperature data from the measured node points to the cutting zone.

4.1. Experiment grinding configuration of thermocouples for measuring the temperature

An equally-spaced array of 6 thermocouples was placed in the upper surface (Figure 10), three on each side, symmetric to the cutting tool position. This positioning ensures reliable experiment results. Another two thermocouples were placed on the lower surface.

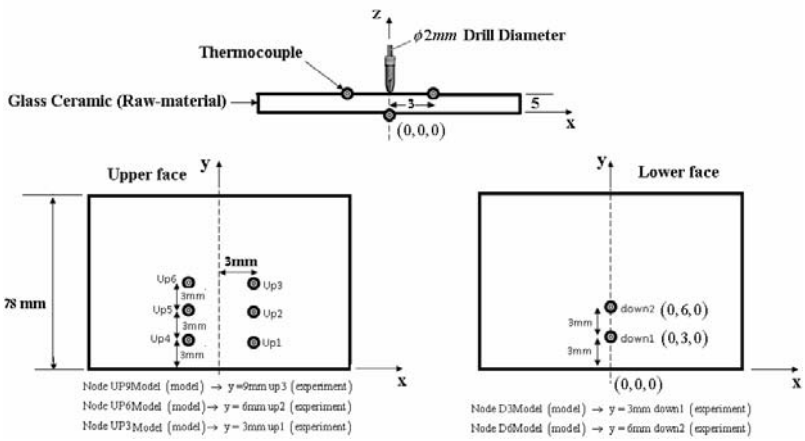

Figure 10. Experiment grinding configuration of thermocouples for measuring the temperature.

4.2. Description of the mesh and the boundary conditions in the grinding model

Due to the symmetry of the problem in terms of geometry, loads (heat moving sources) and boundary condition (there is no convection across the symmetrical plane and on the moving heating sources) we built a half-plate model and thereby save calculation time. A fine-mesh was built near the heat moving sources to capture the delicate changes (Figure 11).

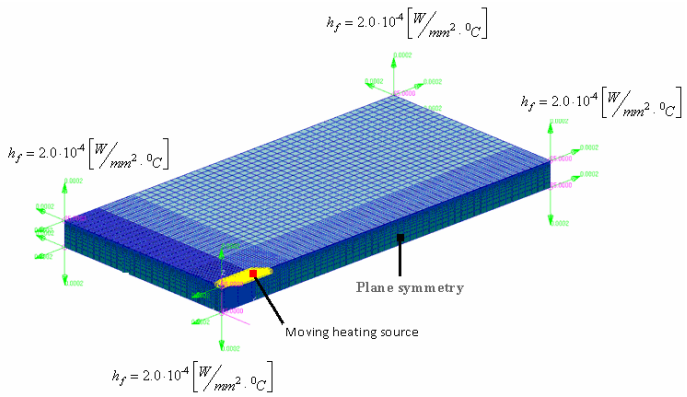

Figure 11. Boundary conditions for half a grinding model with fine mesh near the heat source

4.3. Description of the heat sources in the grinding model without cooling

The grinding area is located on the center of the upper surface of the plate. The grinding is executed from the center of the edge towards the center of the plate for a distance of 8 mm (the yellow strip in Figure 11). In the experiment the cutting movement is a continuous motion, as for the model, the simulation of the cutting movement is discrete. Along the grinding area a fine mesh was formed and 36 heat sources were placed, all with the same power and same operation time (each one starts to operate after its predecessor stops). The power of the first heat source, which is placed on the edge, increases from zero till half the diameter of the cutting tool penetrated the plate. From this point on its power equals the power of the other heat sources.

4.4. Grinding experiment conditions

The experiment was executed four times with the conditions described below (Table 2)

Table 2. Operational conditions

Parameter	$P_{Machine}\left(Watt\right)$	$n_{Tool}\left(rpm\right)$	$a_{cut}\left(mm\right)$	$V_{Tool}\left(mm/\sec\right)$	$L_{cut}\left(mm\right)$
Value	40	200,000	0.32	0.033	8

4.5. Estimation of the cutting power in the experiment

The experiment system has no power measurement system. Therefore, the value of cutting power was based on specific cutting energy (U), known from the literature and the calculation of MRR that depends on the cutting parameters (depth and width of cut, feed rate). U depends on the depth of the cut. The MRR value is calculated in Eq. (1) and the cutting power is calculated in Eq. (2).

$$MRR\left(\frac{mm^3}{\sec}\right)=V_{Tool}\left(\frac{mm}{\sec}\right)\cdot A_{cut}\left(mm^2\right)\rightarrow A_{cut}=\left(\frac{\pi\cdot d_{Tool}}{2}\right)\cdot\left(a\right)=\left(\frac{\pi\cdot 2}{2}\right)\cdot\left(0.32\right)=1.0mm^2 \tag{1}$$

$$MRR=0.033\left(\frac{mm}{\sec}\right)\cdot 1.0=0.033\left(\frac{mm^3}{\sec}\right)$$

$$P_{cut}=U\left(Watt\cdot Sec/mm^3\right)\cdot MRR\left(\frac{mm^3}{\sec}\right)=30\cdot 0.033=1.0\left(Watt\right) \tag{2}$$

The estimated value of the cutting power is 1 Watt for the full plate.
Given half a plate in the model, 0.5 Watt was entered to the grinding model as the thermal power.

4.6. Experiment results versus grinding model results

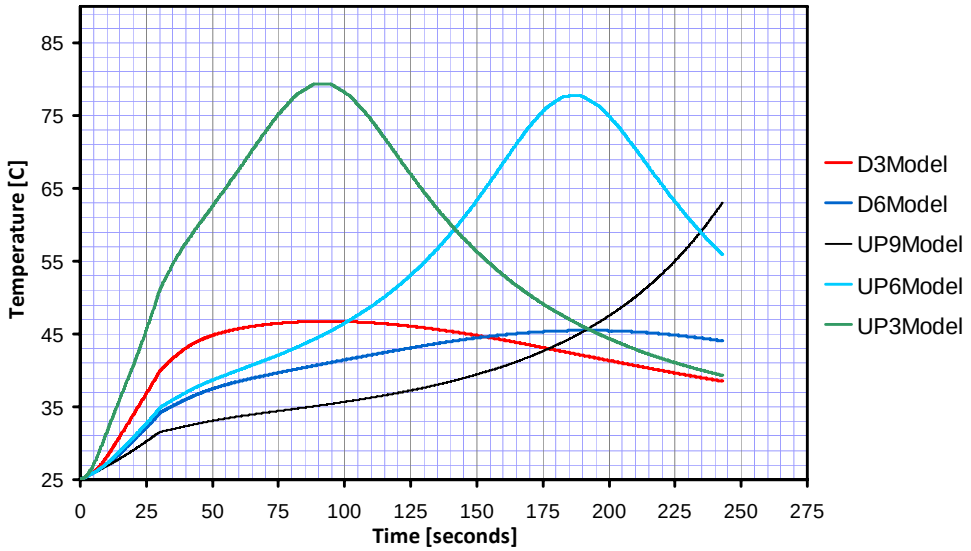

Figure 12. Half model temperature results versus time of five thermocouples

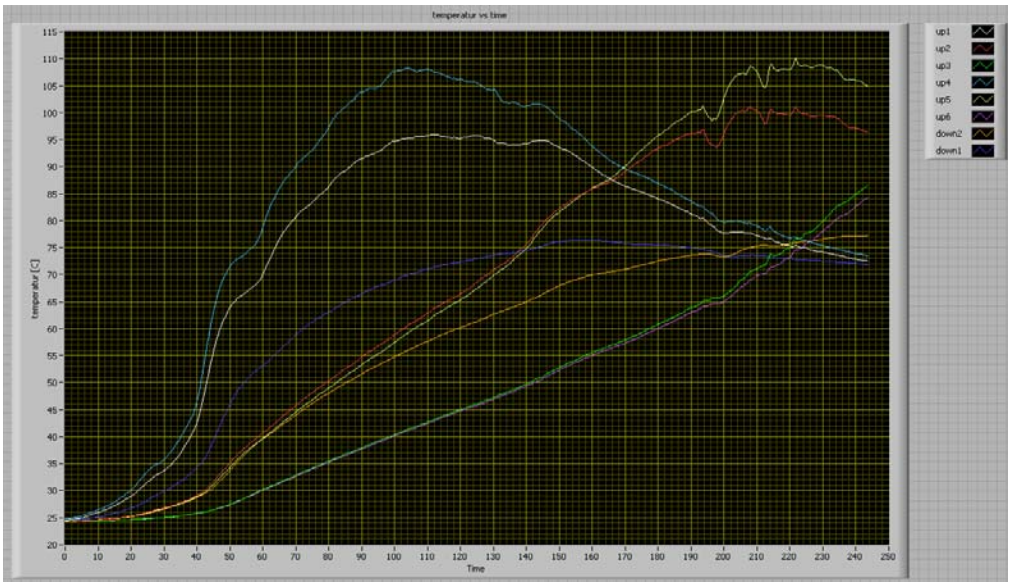

Figure 13. Experimental temperature results versus time of eight thermocouples

5. Results and discussion from Experiment results versus grinding model results

(1) There is a similarity between the graph behaviors of the model to the one of the experiment.

(2) There is a mismatch in the form of the temperature distribution between the model and the experiment, at the first 40 seconds. This is due to the following reasons:

(2.1) Perhaps there is a problem with the adhesive of the thermocouples that causes contact resistance in addition to their thermal mass.

(2.2) It should be noted that in the first 40 seconds the cutting power varies and stabilizes only after the cutting tool penetrates the plates half its diameter.

The objective of this research is to evaluate the temperature around the cutting zone. Due to the low temperatures during the first 40 seconds, the accuracy there is less important.

(3) The temperatures in the experiment are higher by 20% than those of the model. The reason for the difference is that in the model the reaction caused by the contact of the cutting tool lower edge with the plate was neglected. This difference can be solved by executing peripheral milling. Another reason for the gap is the high value of depth of cut (0.32 mm) in grinding. Using a lower value will reduce the temperature gap.

Future work will further develop power measurement in the experiment by measuring the electrical power (Volt, Ampere) or by measuring the torque and the rpm of the rotating cutting tool.
Further experiments will be held with a variety of depths of cut (25, 50, 100, and 150 μm).
The specific cutting energy (U) can by calculated by measuring the cutting power from the experiment and dividing by the calculate MRR. In this case the temperature measurement is unnecessary.

Acknowledgement:

This research was supported by a grant from the ORT Braude College research committee & The Ministry of Industry in Israel.

References

[1] D.A. Stephenson, Tool-Work Thermocouple Temperature Measurement, Trans. ASME.J. Eng. Ind. (1993) 432-437.
[2] D.A. Stephenson, Assessment of steady state metal cutting temperature models based on simultaneous infrared and Thermocouple data, Trans. ASME.J. Eng. Ind. (1991) 121-128.
[3] G..S. Reichenbach, Experimental Measurement of metal cutting temperature distributions, Trans. ASME.J. (1958) 525-546.
[4] G. Boothroyd, Photographic technique for the determination of metal cutting temperatures, Br. J. Applied Physics. 12 (1961) 238-242.
[5] M. Regev, H. Judes, U. Ben-Hanan, Wear Mechanisms of Diamond Coated Dental Burs, Tribology - Materials, Surfaces & Interfaces, (2010) 38-42
[6] N. Bianco, O. Manca, S. Nardini, Comparison between Thermal Conductive Models for Moving Heat Sources in Material Processing, ASME HTD, 369-6. (2001) 11-22.
[7] N. Bianco, O. Manca, V. Naso, Numerical analysis of transient temperature fields in solids by a moving heat source, HEFAT2004, 3rd Inte. Conf. on Heat Transfer, Fluid Mechanics and Thermodynamics, Paper n. BN2, 21 – 24 June 2004, Cape Town, South Africa. 2004.
[8] D.A. Doman, A. Warkentin, R. Bauer, Finite element modeling approaches in grinding, International Journal of machine tools and manufacturing, (2009) 109-116.
[9] J.O. Outwater, M.C. Chaw, Surface temperatures in grinding, ASME Transactions, (1952) 74(1) 73-81.
[10] X. Xu, S. Malkin, Comparison of methods to measure grinding temperatures, Journal of Manufacturing science and engineering, (2001).191-195.
[11] C. Milton Shaw, Metal cutting principle, UK Oxford University Press, London, 2005
[12] G. Bootthrody, Fundamentals of Metal Machining and Machine Tools, McGraw-Hill, New York, 1981.
[13] TW. Hwang, CJ. Evans, S. Malkin, Size effect for specific energy in grinding of silicon nitride. Wear, (1999) 225: 862–867.
[14] TW. Hwang, S. Malkin, Upper bound analysis for specific energy in grinding of ceramics. Wear, (1999) 231: 161–171.